Available online at www.sciencedirect.com
ScienceDirect
Journal of the European Ceramic Society 30 (2010) 3041–3046
www.elsevier.com/locate/jeurceramsoc

Recovery strain of ceramics during sintering

Olivier Guillon *, Jean-Baptiste Ollagnier

Institute of Materials Science, Technische Universität Darmstadt, Petersenstr. 23, D-64287 Darmstadt, Germany

Received 24 August 2009; received in revised form 28 May 2010; accepted 19 June 2010
Available online 16 July 2010

Abstract

A recovery strain after compressive loading was observed for bulk ceramic specimens during sintering. For pure alumina and low temperature co-firing ceramic (LTCC), a transient expansion occurs only in the loading direction after rapid removal of the load. This effect increases with stress magnitude and loading time.

Keywords: Recovery; Sintering

1. Introduction

The phenomenon of anelastic recovery has already been observed for several types of dense ceramic materials, especially composite materials (inert particles in a viscous matrix or liquid phase sintered ceramics), for which particle rotation can have an effect on creep deformation[1]. Morrell and Ashbee[2] have shown that lithium zinc silicate glass-ceramics present after compressive loading an anelastic strain as high as 0.8%. Besson et al.[3] measured a similar behaviour for SiAlYON containing a glassy phase. By noticing the extrusion of glass on the surface of the crept specimens, they proposed that pressure gradients in the grain boundary vitreous phase may lead to glass flow from the high pressure to the low pressure regions and subsequent recovery after unloading. Studies on hot-pressed silicon nitride[4] or Si_3N_4/MgO alloys[5] have shown that the recoverable strain is linearly related to the stress applied on the specimen prior to unloading. It was argued that recoverable creep originated from residual stresses due to contact asperities at grain boundaries hindering grain boundary sliding.

Recovery has also been mentioned for reinforced alumina. For example, four-point bending test were carried out at 1450 °C on silicon carbide-whisker-reinforced alumina.[6] It appears that with 15 vol.% whiskers a large recovery strain is achieved, which is independent of the total creep strain at which the load is removed. As alumina with a lower content of reinforcing elements did not show any significant recovery effect, it seems that a critical volume fraction is required to form an interconnecting whisker network.[7] Large amount of elastic energy can indeed be stored between whiskers due to Hertz contact. On the other hand, large time-dependent strain recovery has been observed by Todd[8] on superplastic metallic alloys. If the long relaxation time regime (which takes place during several hours after unloading) can be explained by a grain shape change by grain boundary diffusion and driven by grain boundary tension, the reasons for short relaxation time anelasticity remain unclear.

Recovery was modelled phenomenologically by using assemblies of uniaxial rheological elements, such as spring and dashpots in parallel or in series with respect to the applied stress.[2,9] As often seen for real materials, a network of such elements with adequate constants (relaxation times) is required in order to get realistic simulations. This descriptive approach, however, does not give any details at the microscopic scale. More recently, Wei et al.[9] investigated through numerical simulations the effect of heterogeneous diffusivity in polycrystalline materials at the scale of individual grains. As atoms could flow easily along paths of high diffusivity and be blocked by low diffusivity grain boundaries, transient effects (local tensile or compressive stress after the macroscopic load has been removed) may lead to inelastic deformation which can be partially recoverable.

Experimental observation of recovery has not been reported for single-phase ceramics densifying by solid state diffusion or Low Temperature Co-fired Ceramics (LTCC). Thus in this paper the time-dependent recovery behaviour of a porous alumina and

* Corresponding author. Tel.: +49 06151 166396; fax: +49 06151 166314.
E-mail address: guillon@ceramics.tu-darmstadt.de (O. Guillon).

0955-2219/$ – see front matter © 2010 Elsevier Ltd. All rights reserved.
doi:10.1016/j.jeurceramsoc.2010.06.009

LTCC glass ceramic composite during sintering was characterized experimentally as function of the applied load. Possible theoretical basis are discussed to rationalize these results.

2. Experimental procedure

2.1. Alumina

An ultrafine and pure alumina powder was used (TM-DAR, Taimei Chemical, Tokyo, Japan; mean particle size 150 nm, 99.99% Al_2O_3). Cylindrical specimens were first pressed using a uniaxial pressure of 100 MPa and then consolidated by 250 MPa in a cold isostatic pressing step. Final shape was ~20 mm height and 11.7 mm diameter (green relative density 57.0%). Specimens were heated at 30 °C/min up to 1200 °C in a sinter-forging apparatus.[10] A thermocouple placed near the specimen provided reliable temperature measurement and control. Above 1000 °C (temperature for which densification starts), a uniaxial compressive load was linearly increased up to 2150 N or 4300 N, with a rate of 360 N/min or 720 N/min, respectively, until reaching the temperature plateau (corresponding to a stress of 20 or 40 MPa, respectively). The applied load was kept constant until a density of ~87.5% was reached. The specimen was then quickly unloaded within 2 s and further maintained at a constant temperature of 1200 °C. Strains were continuously recorded, as radial and axial shrinkages were measured in situ with two orthogonal laser scanners.[10] The average over 64 scans was recorded every 2 s; this time interval was chosen as a compromise between accuracy and timely resolution. Density could be determined during the entire cycle.

Additional experiments were done as follows:

(i) short loading testings: specimens were freely sintered with the same heating program until 87.5% of density, then quickly loaded with a rate of 4000 N/min up to 2150 N. The maximal load was held 5 s and then released like for the normal recovery experiments.
(ii) loading of dense specimens: dense specimens (sintered previously at 1350 °C for 2 h) were heated up to 1200 °C, loaded up to 20 MPa (load adjusted to the current cross-section) with a rate of 360 N/min for 5 min and then quickly unloaded.

2.2. LTCC

For LTCC materials, the commercial Ceramtape GC (CeramTec AG, Plochingen, Germany) was used. It consists of a calcium aluminosilicate glass with an alumina ceramic filler. Proportion of alumina particles is 43% by weight (~35 vol.%).[11] Cylindrical specimens were uniaxially dry pressed at 150 MPa for 20 s and then cold isostatically pressed at 700 MPa for 1.5 min. Green bodies had the following dimensions: 16.85 ± 0.05 mm in height and 11.44 ± 0.03 mm in diameter, with a relative green density of $68.0 \pm 0.2\%$.

Samples were heated up at 30 °C/min and then sintered at 840 °C in the above-mentioned sinter-forging apparatus. Contrary to experiments conducted on alumina, the applied uniaxial stress was adjusted to eliminate the shrinkage in the radial direction and therefore varied as densification proceeded.[12] The applied uniaxial stress was coupled with the measured radial strain. This mode was activated as soon as the sample began to shrink. Both radial and axial strains as well as the uniaxial load maintaining the zero radial strain were recorded simultaneously. Specimens were quickly unloaded after reaching 80%, 85%, 90% and 95% of relative density.

An additional experiment was conducted on a nearly dense sample (99.5%). A constant load of 50 N was applied during 120 s and then quickly released.

Table 1
Recovery strain and time as function of applied pressure for alumina samples.

Stress (MPa)	Total strain	Elastic strain	Anelastic strain	Recovery time (s)
20	1.70×10^{-3}	7.81×10^{-5}	1.62×10^{-3}	80
40	3.31×10^{-3}	1.44×10^{-4}	3.17×10^{-3}	110

3. Results

3.1. Alumina

Typical true strain curves for alumina are presented in Fig. 1. First, during heating the thermal expansion behaviour is isotropic until 1000 °C. As soon as densification takes place and the uniaxial load is applied, the axial strain rate is increased whereas the radial one is decreased, as predicted by the well-known continuum mechanical constitutive laws.[13] As a consequence, a true strain of more than 33% is reached axially, whereas the radial shrinkage is reduced to less than 4%. Fig. 1(b) and (c) show a zoomed view in the vicinity of the load removal. In the radial direction, only a change of slope can be observed: as free sintering can take place, radial shrinkage rate is increased and the specimen continues densifying. On the other hand, it appears that a rapid elongation of the specimen occurs in the axial direction. This recovery develops during about 1 min until macroscopic densification becomes again predominant.

In order to analyze this behaviour, the average total recovered strain was calculated from the data of three specimens (Table 1). It is defined as the difference between the last point under loading and the asymptotic strain level. Similarly the recovery time was taken between these two points. At that temperature and density, the sintering body is viscoelastic, and this total strain can be decomposed into an elastic part and an anelastic part. To calculate the elastic strain at 1200 °C as function of density, the following relationship for the Young's modulus of porous alumina was used[14,15]:

$$E(T, \rho) = E_0(T) \times \left(1 - \frac{P}{P_0}\right)^n \quad \text{with}$$
$$E_0(T) = 417 - 0.0525T \text{ GPa} \quad \text{and}$$
$$P_0 = 0.395 \text{ and } n = 1.15 \tag{1}$$

where T is the temperature and P the porosity.

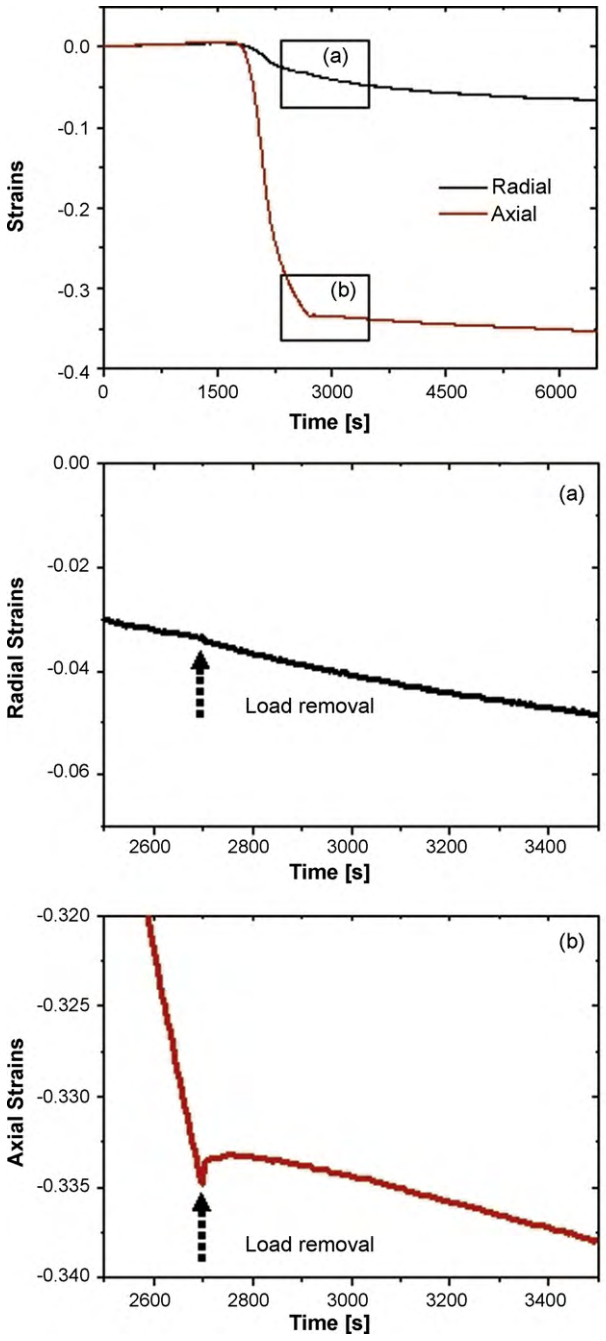

Fig. 1. Typical true strain curves obtained from recovery tests during sintering at 1200 °C (pure alumina, applied stress: 20 MPa).

The measured recovery strain is moderate, but more than one order of magnitude larger than the elastic strain. It is quasi-proportional to the applied stress, which may be related to the fact that grain boundary diffusion controls densification during hot forging (stress exponent of 1).[16] Recovery times ranged from about 1 to 2 min and increased with applied stress. It is interesting to note that for all experiments done, no recovery effect could be measured in the radial direction.

As a comparison, short loading testings produced an anelastic recovery strain of 4.62×10^{-4} and experiments on dense specimens of 5.55×10^{-4}. Both values are less than the elastic strain

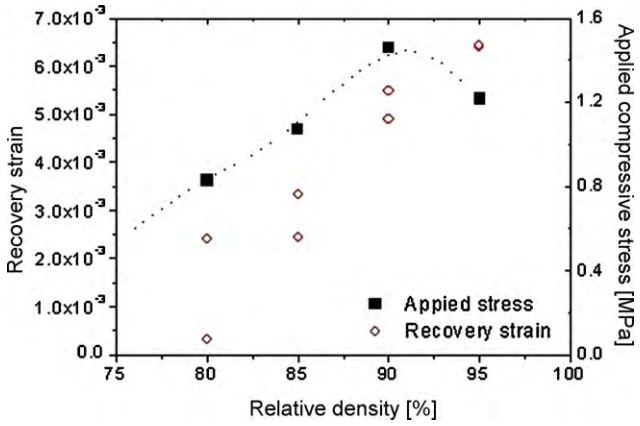

Fig. 2. Recovery strain and applied compressive stress for LTCC as a function of density (zero radial shrinkage sinter-forging).

and about 3 times smaller than that of standard specimens. In the case of dense specimens, recovery times are very long (about 1000 s).

3.2. LTCC

As indicated previously and depicted in Fig. 2, the compressive stress required to maintain the zero radial shrinkage varies as densifications proceeds: it increases up to ~90% of relative density and then decreases. After removal of the load, the recovery strain depends both on the loading history and the degree of densification. As the applied stress increases, the recovery strain increases. Moreover, as the densification proceeds, the recovery strain increases even though the magnitude of the load before removal is lower. The scattering of the axial strain increase at low densities can attributed to the poor control of the load. At low densities, strain rates are high and drop significantly as densification proceeds. Therefore, adjustment of the load is more difficult at lower densities than at higher densities.

The part of the elastic strain in the recovery strain has also been evaluated for the different experiments. Elastic properties of the LTCC material as a function of temperature and density were previously measured and reported elsewhere.[17] The Young's modulus of LTCC at a temperature of 840 °C varies between 33 GPa and 81 GPa, for a sample having a relative density of 80% and a dense sample, respectively. Due to the very low magnitude of the applied stresses (0.8–1.5 MPa) the elastic strains for the zero shrinkage experiments remained small: 1.8×10^{-5} and 2.5×10^{-5} for 95% and 80% of relative density, respectively. Therefore, elastic strains are negligible compared to the recovery strain (in the range of $3.1. \times 10^{-4}$ to 6.4×10^{-3}).

Recovery time as a function of the degree of densification has also been investigated (Fig. 3). Recovery time increases significantly with density. Recovery time is small at low densities since strain rates are very high. It can be seen as a competition between recovery effect and further densification, if these processes are independent of each other. At low densities, the densification is the predominant phenomenon whereas at high densities, where strain rates are small, the recovery effect prevails.

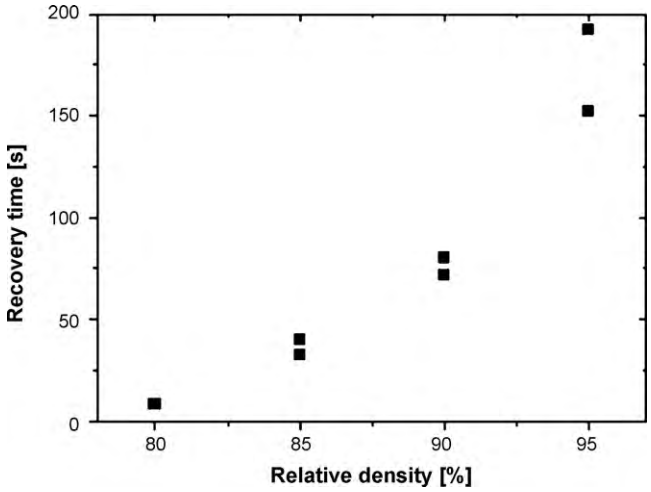

Fig. 3. Recovery time for LTCC as a function of density (zero radial shrinkage sinter-forging).

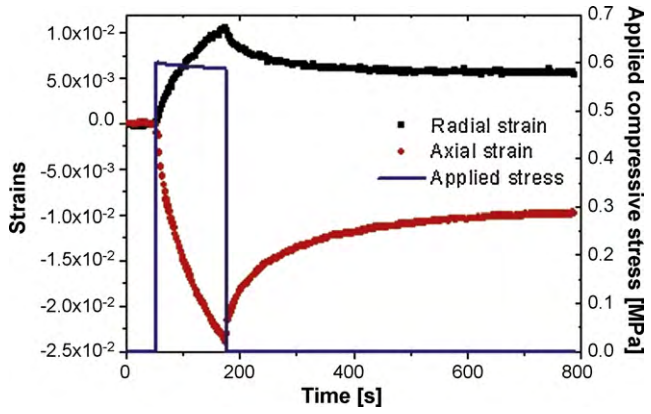

Fig. 4. Strain and loading curves for nearly dense LTCC as a function of time.

Finally, an additional loading test was carried out on a nearly dense LTCC sample of 95.5% of relative density. Strains and applied stress are plotted in Fig. 4. The nearly dense sample at the temperature of 840 °C did not show any further densification since the axial and radial strains remained equal to zero until the application of the load. It is also interesting to notice that the density remained identical after unloading. Since the diameter expands under the constant loading, the applied stress decreases from 0.6 MPa to 0.587 MPa during the loading period. After quick removal of the load, a recovery strain as high as 1.4×10^{-2} has been recorded. It is about twice as much as the recovery strain measured after 95% of relative density. As before, the elastic part of the recovery strain is negligible (7.4×10^{-6}). Similar to alumina, the recovery time for nearly dense LTCC samples is longer than for sintering bodies and was found to be about 600 s.

4. Discussion

As the presence of a liquid or viscous phase as well as high stiffness inclusions can be excluded due to the high purity of the alumina used, a plausible reason for this recovery has to be found. Recovery increases with the applied stress and is significantly reduced when either the stress is applied for a short time or when densification is exhausted. The phenomenon of desintering occurs locally between dense and porous regions or between inclusion and densifying matrix.[18] Due to gradients in green density or heterogeneities in the packing, polycrystalline bridges can be broken locally. However, it is difficult to imagine this effect playing a significant role after hot forging of homogeneous bulk specimens. When using classical continuum mechanical equations in cylindrical coordinates,[13]

$$\dot{\varepsilon}_y = \dot{\varepsilon}^{free} + \left(\frac{1}{E_p}\right)[\sigma_y - \nu_p(\sigma_r + \sigma_\theta)] \quad (2)$$

a positive axial strain rate $\dot{\varepsilon}_y$ is only possible when a tensile stress σ_y is large enough to counteract the free sintering strain rate $\dot{\varepsilon}^{free}$, or when normal stress components σ_r or σ_θ act through Poisson's effect (E_p is the uniaxial viscosity and ν_p is the viscous Poisson's ratio). This framework can therefore not explain the present results. In addition, microscopic models[19,20] using a simplified unit cell (typically two spherical particles joined by a flat circular grain boundary) can predict the plating rate of these particles under a compressive stress. The uniaxial pressure increases the gradient in vacancy concentration along the grain boundary, increasing the atom flux and strain rate while interparticle neck grows. Stress removal does not induce any change in the direction of particle relative motion, only its intensity. In order to stop densification, vacancy gradient has to be zero; in order to get an elongation of the unit cell, this gradient has to be reversed, namely more vacancies in the centre of the neck than at the solid/vapor interface. In summary, classical isotropic approaches cannot account for this effect.

It has been previously shown that a load of several MPa applied on alumina during sintering can affect the macroscopic densification behaviour by inducing an anisotropic microstructure.[21–23] It was proposed that necks grow faster under compression that those parallel to the load, which induces elongated pores in the direction of the loading and eventually elongated grains if grain growth takes place. Such an anisotropic microstructure may be the reason for the observed transient recovery. During subsequent free sintering, it is also expected that the degree of anisotropy decreases and the microstructure tends to be isotropic.[22,23] But even stress induced anisotropic material is not expected to expand when applying constitutive equations.

However, in the case of an early asymmetric two-particle model, Exner and Bross[25] showed that different pore curvatures lead to an asymmetric stress state along the grain boundary. A non-symmetry in the grain boundary stress results in removal of atoms at one boundary/pore interface and deposition at the other one. This may lead to particle rearrangement (tilting) and to an increase of the macroscopic axial strain. Related to the present results, one could consider that the mechanical load would create more asymmetric necks by promoting particle rearrangement. This agrees with the proposition of Cocks,[24] who argued that a constrained film during sintering should expand along its thickness if suddenly released from its substrate. To observe experimentally this effect, a switch between constrained and free sintering conditions at high temperature should be pro-

vided or at least very high cooling and re-heating rates made available, in order to minimize microstructure evolution due to surface diffusion and further densification.

On the other hand, three-dimensional modelling as proposed by Svoboda et al.[26,27] enabled to compute the sintering stress for an open and closed isotropic periodic structures. The sintering stress is defined as the mechanical hydrostatic stress which balances the internal surface tension forces, reducing thereby the volume change to zero. They found interestingly that the sintering stress can become negative for small values of the dihedral angle, which means that no further densification occurs for that type of material beyond a given density. This result was recently confirmed by Wakai[28,29]. He proved by different methods (energy, force balance and volume averaging) on isotropic as well as anisotropic packings that the sintering stress components are always positive except for low dihedral angle and high densities. Nevertheless, one should keep in mind that a condition to get an elongation in one direction does not necessarily involve desintering and a negative hydrostatic sintering stress. All sintering stress tensor components are indeed involved, weighted by anisotropic uniaxial viscosities and viscous Poisson's ratios. As a proof of this, the relative density of the specimens experiencing recovery never decreased. The axial strain is indeed compensated by the larger radial shrinkage.

The LTCC material investigated here contains significantly more viscous phase than others already presented in the literature (maximal 20%[2,3]), but still reversible extrusion of glass could be the reason for recovery. As recovery strain increases with density, it is assumed that remaining pores are detrimental to this phenomenon. During continuous sinter-forging experiments it has been previously observed that pores tend to elongate perpendicularly to the load, as they remained attached to elongated alumina particles.[30] Thus reorientation under load of alumina particles may push some viscous phase out of the interparticle contact areas. After load release, glass intrusion may take place, giving rise to a partially reversible movement of alumina particles and macroscopic elongation of the specimen.

On the other hand, according to Olevsky,[31] a spheroidization of ellipsoidal pores can take place and this leads to a swelling in the direction of smaller axis. It was further established that the LTCC porous body recover its pseudo-isotropic state shortly after the removal of the load by comparing the subsequent free sintering of loaded with unloaded samples.[32] To check experimentally this hypothesis in relation to recovery, samples made of pure glass mixed with pore formers (for instance polystyrene balls) could be sintered, leaving large isolated pores in a dense matrix. Investigation of pore shape during and after loading by in situ microtomography could be correlated to the macroscopic strains.

5. Conclusions

In this paper, a recovery strain was observed for pure alumina and LTCC bulk specimens, densifying by grain boundary diffusion and viscous flow, respectively. After rapid removal of the load, a transient expansion occurs only in the loading direction. Its amplitude increases with the stress magnitude and loading time. Whereas for pure alumina recovery decreases significantly for higher densities, the recovery strain is maximized for dense LTCC. Although no quantitative modelling can be proposed, the development of anisotropy under load is thought to be responsible for that behaviour.

Acknowledgements

Fruitful exchanges with J. Rödel, D. Green, R. Bordia have been greatly appreciated. This work was partly financially supported by the Deutsche Forschungsgemeinschaft (DFG) through the Emmy Noether program (Gu 993-1).

References

1. Wilkinson DS. Creep mechanisms in multiphase ceramic materials. *J Am Ceram Soc* 1998;**81**(2):275–99.
2. Morrell R, Ashbee KHG. High temperature creep of lithium zinc silicate glass-ceramics. *J Mater Sci* 1973;**8**:1271–7.
3. Besson JL, Streicher E, Chartier T, Goursat P. Viscoelastic creep of nitrogen ceramics. *J Mater Sci Lett* 1986;**5**:803–5.
4. Arons RM. PhD thesis. Columbia University, School of Engineering and Applied Science; 1978.
5. Lange FF, Clarke DR, Davis BI. Compressive creep of Si_3N_4/MgO alloys. Part 2. Source of viscoelastic effect. *J Mater Sci* 1980;**15**:611–5.
6. Gu W, Porter JR, Langdon TG. Evidence for Anelastic creep recovery in silicon carbide-whisker-reinforced alumina. *J Am Ceram Soc* 1994;**77**(6):1679–81.
7. Quan GC, Conlon KT, Wilkinson DS. Investigation of anelastic creep recovery in SiC whisker-reinforced alumina composites. *J Am Ceram Soc* 2005;**88**(11):3104–9.
8. Todd RI. Grain boundary tension induced strain recovery following superplastic flow. *Acta Metall Mater* 1994;**42**(9):2921–8.
9. Wei Y, Bower AF, Gao H. Recoverable creep deformation and transient local stress concentration due to heterogeneous grain-boundary diffusion and sliding in polycrystalline solids. *J Mech Phys Solids* 2008;**546**:1460–83.
10. Aulbach E, Zuo R, Rödel J. Laser-assisted high-resolution loading dilatometer and applications. *Exp Mech* 2004;**44**(1):71–5.
11. Rauscher M, Roosen A. Influence of low-temperature co-fired ceramics green tape characteristics on shrinkage behaviour. *Int J Appl Ceram Technol* 2007;**4**(5):387–97.
12. Zuo RZ, Aulbach E, Rödel J. Shrinkage-free sintering of low-temperature co-fired ceramics by loading dilatometry. *J Am Ceram Soc* 2004;**87**(3):526–8.
13. Bordia RK, Scherer GW. On constrained sintering. 1. Constitutive model for a sintering body. *Acta Mater* 1988;**36**(9):2393–7.
14. Munro RG. Evaluated material properties for a sintered α-alumina. *J Am Ceram Soc* 1997;**80**(8):1919–28.
15. Ostrowski T, Ziegler A, Bordia RK, Rödel J. Evolution of Young's modulus, strength, and microstructure during liquid-phase sintering. *J Am Ceram Soc* 1998;**81**(7):1852–60.
16. Rahaman MN. *Ceramic processing and sintering*. New York: Marcel Dekker; 2003.
17. Ollagnier J-B. Constraint and anisotropy during sintering of a LTCC material. PhD; 2008.
18. Sudre O, Lange FF. The effect of inclusions on densification. III. The desintering phenomenon. *J Am Ceram Soc* 1992;**75**(12):3241–51.
19. Zhang W, Schneibel JH. The sintering of two particles by surface and grain boundary diffusion—a two-dimensional numerical study. *Acta Metall Mater* 1995;**43**(12):4377–86.
20. Bouvard D, McMeeking RM. Deformation of interparticle necks by diffusion-controlled creep. *J Am Ceram Soc* 1996;**79**(3):666–72.

21. Zuo R, Aulbach E, Bordia RK, Rödel J. Critical evaluation of hot forging experiments: case study in alumina. *J Am Ceram Soc* 2003;**86**(7):1099–105.
22. Bordia RK, Zuo R, Guillon O, Salamone SM, Rödel J. Anisotropic constitutive laws for sintering bodies. *Acta Mater* 2006;**54**:111–8.
23. Wonisch A, Guillon O, Kraft T, Moseler M, Riedel H, Rödel J. Stress-induced anisotropic behaviour of sintering alumina: discrete element modelling and experiments. *Acta Mater* 2007;**55**(15):5187–99.
24. Cocks ACF. Sintering of constrained films. In: *International Conference on Sintering*. 2008.
25. Exner HE, Bross P. Material transport rate and stress distribution during grain boundary diffusion driven by surface tension. *Acta Metall* 1979;**27**:1007–12.
26. Svoboda J, Riedel H, Zipse H. Equilibrium pore surfaces, sintering stresses and constitutive equations for the intermediate and late stages of sintering—I. Computation of equilibrium surfaces. *Acta Metall Mater* 1994;**42**(2):435–43.
27. Riedel H, Zipse H, Svoboda J. Equilibrium pore surfaces, sintering stresses and constitutive equations for the intermediate and late stages of sintering—II. Diffusional densification and creep. *Acta Metall Mater* 1994;**42**(2):445–52.
28. Wakai F. Modeling and simulation of elementary processes in ideal sintering. *J Am Ceram Soc* 2006;**89**(5):1471–84.
29. Wakai F, Shinoda Y. Anisotropic sintering stress for sintering of particles arranged in orthotropic symmetry. *Acta Mater* 2009;**57**:3955–64.
30. Ollagnier J-B, Guillon O, Rödel J. Effect of anisotropic microstructure on the viscous properties of an LTCC material. *J Am Ceram Soc* 2007;**90**(12):3846–51.
31. Olevsky E, Skhorokod V. Deformation aspects of anisotropic-porous bodies sintering. *J Phys* 1993;**3**(C7):739–42.
32. Ollagnier J-B, Guillon O, Rödel J. Viscosity of LTCC determined by discontinuous sinter-forging. *Int J Appl Ceram Technol* 2006;**3**(6):437–41.